J. Indian Chem. Soc.,
Vol. 96, August 2019, pp. 1059-1065

Effect of surface treatment on photovoltaic properties of dye-sensitized solar cell based on natural dye quercetin

Giriraj Chayal[a]*, Kharta Ram Patel[a], Mahesh Saran Roy[b], Manish Kumar[b], Narottam Prasad[b] and Kirti Shitiz[b]

[a]Department of Physics, J. N. V. University, Jodhpur-342 005, Rajasthan, India

E-mail: chayal.physics@gmail.com

[b]Defence Laboratory, Ratanada, Jodhpur-342 011, Rajasthan, India

Manuscript received online 29 November 2018, revised and accepted 26 July 2019

In this study, the effects of surface treatments of working anode with co-adsorbents such as chenodeoxycholic acid (CDCA) and $TiCl_4$ over efficiency and other photovoltaic parameters of dye-sensitized solar cell (DSSC) have been observed. The DSSC based on natural dye quercetin as sensitizer using quasi-solid polymeric electrolyte was fabricated. The improvement in power conversion efficiency (η) from 0.13% to 0.35% was well justified by increment in various photovoltaic parameters such as open circuit voltage (V_{oc}), short circuit density (I_{sc}) and fill factor (FF). The overall increment in power conversion efficiency after CDCA + $TiCl_4$ treatment was found to be around three times of the efficiency of untreated device. The use of polymeric electrolyte system consisting of I^-/I_3^- redox moieties imparts stability to the devices, which is essential for the commercial potential.

Keywords: Quercetin, nano crystalline TiO_2, DSSC, quasi solid polymeric electrolyte.

Introduction

The dye-sensitized solar cell includes a metal oxide semiconductor (generally TiO_2 or ZnO) porous film coated on fluorine doped tin oxide (FTO), dye or photosensitizer, a redox electrolyte (generally triiodide/iodine) and a counter electrode[1]. The major breakthrough was made by Grätzel *et al*. in 1991 who reported the DSSC structure consisting of inorganic semiconductor films nano crystalline TiO_2 sensitized with a trimeric ruthenium complex[2]. The improvement in the efficiency of DSSCs requires reduced charge recombination and increased electron injection efficiency, which are closely linked to the open-circuit photovoltage (V_{oc}). To improve the V_{oc}, various efforts have been made such as modification in sensitizer[3] use of co-adsorbents[4], novel redox couples[5] and additives[6].

The performance is also badly affected by the dye aggregates formed on the semiconductor surface[7,8]. Dye aggregation may lead to reduction in electron injection, giving rise to low photo current. Since dye aggregation leads to the intermolecular quenching or molecules residing in the system not functionally attached to the TiO_2 surface, therefore acts as filter for electron injection, which can also affect the sensitizer regeneration by redox couple[9]. To lessen the dye molecular aggregation, the electron injection efficiency is increased by the addition of co-adsorbents during the sensitizer adsorption[10]. Enhancement in both V_{oc} and the efficiency was observed by the addition of co-adsorbents when the original sensitizers undergo aggregation. The adsorbents forms an additional compacted protection layer on the TiO_2 surface, thereby reducing the charge recombination. Another approach is to enhance the surface area and thus photo current by treatment of TiO_2 layer by $TiCl_4$. This improvement is not only due to increased photo current, but also due to the downward shift in the conduction band edge of the TiO_2 and decline in the electron/electrolyte recombination rate constant[11].

As far as efficiency is considered, highest efficient DSSCs are based on LEG4 + ADEKA-1[12] and inorganic Ru(II) polypyridyl complexes[13]. But due to the shortage of the Ru metal; the ruthenium complexes are expensive. Also the fabrication process of DSSCs based on these metal complexes requires high sophistication. These facts motivated the quest for potential substitute of sensitizers based on metal complex. Various groups have reported DSSCs based on metal

free organic dyes[14–17] and natural dyes[18–23] as photosensitizer. High efficiency (10.3%) DSSC using organic dyes has been reported[17]; however, these dyes suffer some problems, such as complicated synthesis process with low yields. Alternatively natural dyes are being investigated as photo sensitizers in the DSSCs. Though the efficiency of DSSCs based on natural dyes are very low as compared to that of inorganic or synthetic dyes[24], but still they are useful because of low cost, non-toxicity, easy availability in natural resources such as flowers, fruits, leaves, bark etc. and a simple extraction procedure involving organic solvents without the strict requirement of high purity[25]. For the DSSCs based on various natural dyes and TiO_2 nc-crystals, Çetin *et al*. reported FF 0.606 and efficiency 0.067%[26] whereas Bachtiar *et al.* reported efficiencies 0.0183% to 0.0513%[27]. DSSCs based on ZnO photo anode showed low FF 0.20 and efficiency 0.009%[28]. Another group reported FF 0.26 and efficiency 0.013% of DSSC having similar configuration[29]. All these cells were fabricated using liquid electrolyte solution. 1.27% power conversion efficiency of DSSC based on quercetin dye using liquid electrolyte was reported by Özacar *et al.*[30], whereas Sonmezoglu *et al.* reported the conversion efficiency more than 2% with ferrocene electrolyte[31]. However the stability of the devices based on liquid electrolyte is very less. Therefore to improve the stability of the cell, devices were fabricated employing quasi solid polymeric electrolyte.

In the present research work, DSSCs fabricated using natural dye quercetin as photo sensitizer and quasi solid polymeric electrolyte. The effect of photo anode's surface treatments with co-adsorbents by chenodeoxycholic acid (CDCA) and $TiCl_4$ was studied and improvement in all photovoltaic parameters such V_{oc}, J_{sc}, FF and efficiency was observed. The required TiO_2 nano particles were also synthesised in the lab to fabricate the photo anode.

Experimental

Material used:

FTO used as substrate for working as well as counter electrode, was purchased from Sigma-Aldrich with dimensions = L 300 mm×W 300 mm×thickness 3.2 mm and sheet resistivity ~10–12 Ω /sq. It was cut into pieces of dimensions of L 30 mm×W 20 mm×thickness 3.2 mm using diamond cutter. Titanium tetra-n butyl oxide used as precursor to synthesize nc-TiO_2 was purchased from Fluka. H_2PtCl_6 used to fabricate the Pt layer on counter electrode and organic solvent n-methyl pyrrolidone (NMP), gamma butyrolactone (GBL), I_2, KI and polyvinyl butyral (PVB) film used in making of quasi solid state polymeric electrolyte were procured from the Across. Quercetin di-hydrate ($C1_5H_{10}O_7.2H_2O$) was purchased from Himedia. The natural dye quercetin is a yellow crystalline powder and a common dietary flavonol pigment. The structure of quercetin (3,5,7-trihydroxy-2-(3,4-dihydroxy phenyl)-4*H*-chromen-4-one) or (3,3′,4′,5,7-penta hydroxy flavone) is shown in Fig. 1. Quercetin is an antioxidant found naturally in many plants, especially in oak bark, onion skin, radish leaves and tea leaves etc. The molecular weight of quercetin is 302.338 g/mol and molecular formula is $C_{15}H_{10}O_7$.

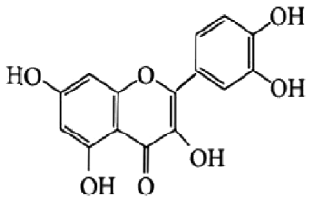

Fig. 1. Chemical structure of quercetin.

Synthesis of TiO_2 nano particles:

To prepare TiO_2 nano powder, we adopted the methodology suggested Li *et al*.[32]. In this procedure titanium tetra-n butyl oxide (TTB) was used as precursor. First of all 40 ml glacial acetic acid and 80 ml of anhydrous ethanol were mixed in 25 ml distilled water (solution-A). Then 34 ml TTB was mixed with 80 ml of anhydrous ethanol under stirring at room temperature (solution-B). Finally solution-B was added drop wise to solution-A under vigorous stirring. The final solution was allowed to stir for 4 h. Then this solution was left for drying at room temperature for 48 h. The material was crushed after drying at 150°C for 2 h. Again this powder was given heat treatment at 450°C for 3 h. Finally this was again crushed to get fine white TiO_2 powder.

Preparation of TiO_2 paste and photo anode:

To prepare screen printable TiO_2 paste, 15 ml n-butanol and 15 ml deionised water were mixed in two different beakers, each containing 3 g of the synthesized TiO_2 nano particles. 1.5 g of ethyl cellulose was mixed with 15 ml n-butanol in another beaker. All three solutions were kept under stirring for 24 h at room temperature. After this all three blend

were mixed together and again left for stirring. After 4 h of stirring, polyethylene glycol (PEG) and turpenol were added in suitable amount and stirring was continued to get homogenised screen printable TiO_2 paste. To prepare nanostructured TiO_2 working electrode, FTO conducting glass was used as substrate. First of all the FTO substrate was cleaned. For cleaning the FTO was sonicated with soap solution, acetone and IPA respectively using ultrasonic bath (Model: Sonicor SG-3042). After this, FTO substrate was put under plasma treatment by using plasma cleaner (Model: Harrick Plasma, PDC-002). After cleaning, the prepared TiO_2 paste was screen printed on FTO substrate to get a smooth thin film. Finally this working electrode was sintered at 450°C for two hours to get smooth interface between TiO_2 and FTO.

Surface treatments:

For sensitization, 20 mM solution of quercetin dye in methanol was prepared. Then fabricated photo (working) anode was immersed in this quercetin solution and left for overnight. Sensitization with quercetin dye was done in three ways, such as without any treatment (Device-D1), after CDCA treatment (Device-D2) and after $TiCl_4$ and CDCA treatment simultaneously (Device-D3). To pre-sensitize the photo anode in chenodeoxycholic acid (CDCA), a 0.1 mM solution of CDCA was prepared in methanol. The prepared photo anode was left in this solution overnight. Then it was dried at room temperature and immersed in quercetin dye for overnight. Another pre-sensitization was carried out with $TiCl_4$ and with CDCA simultaneously. To prepare $TiCl_4$ solution, one ml $TiCl_4$ was added in aqueous solution of 0.1 *M* HCl. The prepared photo anode was first treated with $TiCl_4$ solution for two hours and then rinsed with de-ionized water and left for drying at room temperature. Then again it was pre-sensitized with CDCA as described earlier. Then finally treated photo anode was sensitized with quercetin dye. All sensitized working electrodes are washed with the same solvent (methanol) to remove the excess dye.

Preparation of counter electrode and packing of cell:

To prepare the counter electrode, another FTO conducting substrate was cleaned as described earlier. Meanwhile H_2PtCl_6 was blended with methanol in 1:10 ratio. This solution was coated on cleaned FTO substrate using water bath. Then substrate was sintered at 450°C to get counter electrode.

Before final packing of cell, polyvinyl butyral-based thin film polymeric electrolyte was prepared by using method reported by Chen *et al.*[33]. According to this process, a blend of organic solvent gamma butyro lactone (GBL) and n-methyl pyrrolidone (NMP) was taken in 7:3 volume ratio. Then KI (0.5 mM) and I_2 (0.1 mM) were added to prepare electrolytic solution and left for stirring for 24 h under dark condition to protect from light. Then polyvinyl butyral (PVB) film was immersed into this solution to get quasi solid polymeric electrolyte (SPE) thin film. In the final step, the prepared working and counter electrodes were clamped together sandwiching the SPE thin film to fabricate the dye sensitized solar cell.

Characterizations

The X-ray diffraction pattern (XRD) of the synthesized TiO_2 powder was recorded using PANalytical X'Pert Pro X-ray diffractometer with the incident radiation in the range of 20–70° having a Cu K_α (λ = 1.5406 Å) X-ray radiation with a scan step size of 0.05°/s. This X-ray characterisation was performed at 40 mA and 45 kV of values of current and voltage respectively. Raman spectra of TiO_2 powder was recorded using Raman Instrument (Model: Avlon Instruments, Raman Station R3) using green laser (532 nm) at power 50 mW in the frequency range 200–4000 cm^{-1}.

The optical absorption of the nc-TiO_2 thin film on FTO and dye sensitized photo anode before as well as after surface treatment was recorded in the wavelength range 200–800 nm using UV-Vis spectrophotometer (Model: Specord S 600-analytic jena). The photo response measurement of fabricated DSSC with an active area of 1 cm^2 was carried out with a semiconductor parameter analyzer (Model: HP 4145B) under solar illumination with the incident light having input power 65 mW/cm^2. Various photovoltaic parameters such as open circuit voltage (V_{oc}), short circuit current density (J_{sc}), fill factor (FF) and power conversion efficiency (η) were obtained using J-V curves of different fabricated DSSCs.

Results and discussion

XRD and Raman spectroscopic analysis of synthesized TiO_2:

The XRD pattern of prepared nano TiO_2 is shown in Fig. 2. The XRD pattern reveals that there are six significant diffractive peaks at 25.11°, 37.60°, 47.89°, 53.68°, 54.84° and 62.56° which correspond to six different crystal planes such

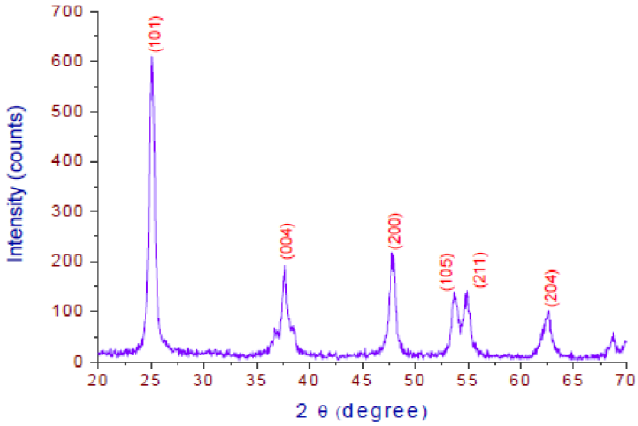

Fig. 2 XRD pattern of synthesised TiO_2 nano particles.

as (101), (004), (200), (105), (211), and (204) respectively. These peaks may be indexed as tetragonal anatase phase of TiO_2 and the diffraction pattern was found to be in good agreement with JCPDS files # 89-4921[34]. The absence of diffraction peaks at 27° and 31° confirms the nonexistence of rutile and brookite phases in the structures of TiO_2[35]. The size of anatase-TiO_2 nanoparticles obtained from the prominent peak (101) at 25.11° using Debye-Scherrer equation was found to be 13.08 nm. The Debye-Scherrer equation is given by $D = k\lambda/(\beta \cos \theta)$, where λ is X-ray wavelength, k is Scherer's factor; β is FWHM and θ being Bragg's angle.

The Raman spectrum of the TiO_2 powder is shown in Fig. 3. It is clear that this spectrum exhibits three strong bands at 400 cm^{-1} (B_{1g}), 520 cm^{-1} (B_{1g}) and 642 cm^{-1} (E_g), which are characteristics peaks of tetragonal anatase-TiO_2[36].

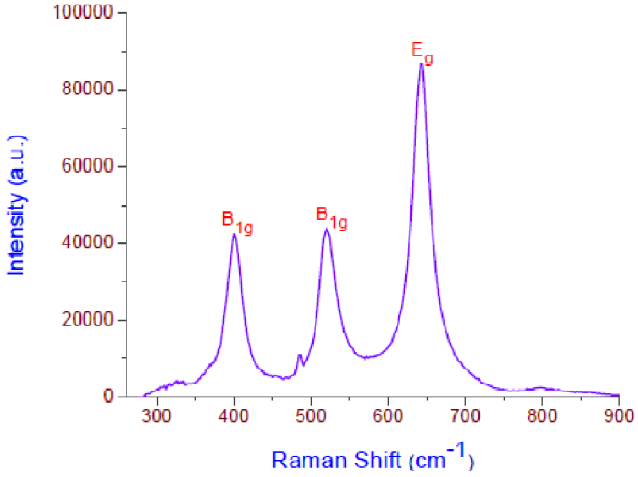

Fig. 3. Raman spectra of synthesised TiO_2 nano particles.

Hence both XRD and Raman analysis indicate the formation of anatase phase of TiO_2 nano particles. Park *et al*. showed that anatase phase is more favourable for electron transport than the rutile phase resulting in better photovoltaic performance[37]. As compared to rutile phase, the anatase phase has larger surface area due to its crystallographic orientation and lower recombination rate due to higher indirect band gap[37,38]. This difference can be attributed to the higher photocurrent in anatase. The value of photo voltage is essentially the same for both the cases.

Optical characterization:

To observe the effect of surface treatments in terms of optical absorption, the normalised UV-Vis spectra of working electrodes before and after pre-treatments were recorded for same range of wavelength (shown in Fig. 4).

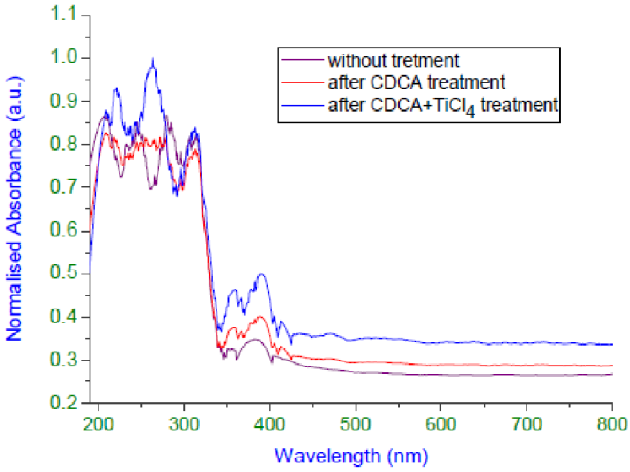

Fig. 4. Normalised absorption spectra of sensitized photo anode in quercetin.

These spectra clearly indicate an improved absorption after surface treatments of photo anode, especially after 350 nm. This enhancement in absorption over a wide range i.e. 350 nm to 800 nm can be attributed to the higher amount of dye loading after surface treatments of working electrodes. The effect of both the co-adsorbent is obvious in absorption as CDCA has been found to reduce the dye aggregation and the $TiCl_4$ provides larger surface area to dye molecules. Both these factors contribute towards higher photo current and reduced charge recombination. This improvement is a critical factor in improving efficiency of the DSSCs. Also to observe whether there is any downward shift in the conduction

band edge of the TiO_2 due to $TiCl_4$ treatment (as reported earlier)[11]; the variation of $(\alpha h\nu)^m$ with $h\nu$ for best fitted an indirect allowed transition for anatase bare and treated TiO_2 thin films were plotted (Fig. 5). Here α is the absorption coefficient calculated using equation $\alpha = (2.303\times A)/d$; where '*A*' is the absorbance and '*d*' is the film thickness taken to be 10 micron. Here $h\nu$ is the photon energy in eV calculated using formula $h\nu = 1240/\lambda$, where λ is the wavelength in nm. The extrapolated value of $\alpha h\nu$ to $\alpha = 0$ gives the band gap 3.6 eV for bare TiO_2 thin film, 3.23 eV for untreated dye sensitized and 3.1 eV for $TiCl_4$ + CDCA treated dye sensitized TiO_2 thin films respectively.

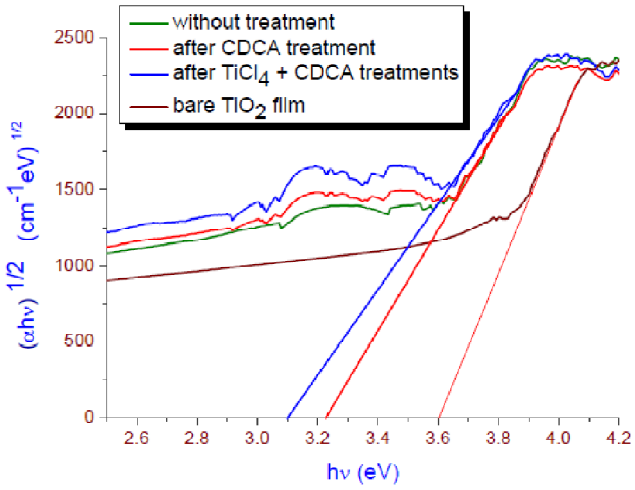

Fig. 5. Indirect transitions for sensitized and bare TiO_2 thin films.

It is explicit that the band gap calculated for the sensitized TiO_2 thin film is lower than the band gap calculated for the crystal structures in synthesized TiO_2. This indicates that sensitization with natural dye quercetin has promoted the band gap narrowing giving rise to increased absorption in longer wavelength region. This is an encouraging property to facilitate the light harvesting in visible range. No difference was observed between band gap values of un-treated and CDCA treated TiO_2 films. It clearly indicates that though the CDCA treatment has improved absorption by reducing dye aggregation; but it has no effect on conduction band of TiO_2. On the contrary, an appreciable lowering in the TiO_2 conduction band was observed after $TiCl_4$ treatment. The $TiCl_4$ has led to the reduction in band gap which manifests the improvement in charge separation efficiency. It can be inferred that this shift in conduction band edge has led enhancement in current which resulted due to improved charge injection into the TiO_2.

Photovoltaic properties:

The J-V characteristics of the fabricated DSSCs are shown in Fig. 6. It is quite clear that surface treatments have led to the enhancement in short circuit current density J_{sc}. This is due to reduced dye aggregation and increased charge injection into the TiO_2. Transparent organic compound CDCA obstructs the dye aggregation; because it strongly gets attached to the TiO_2 surface and dislodges the dye molecules[39].

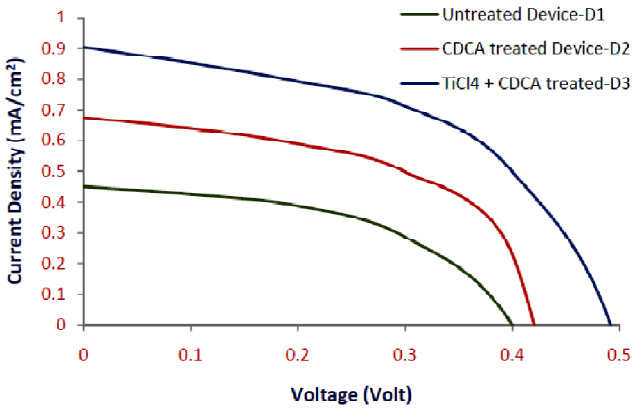

Fig. 6. Current density vs voltage curves of fabricated DSSCs.

This hindrance in dye aggregation, results in enhanced electron injection efficiency, which leads to an improvement in the photocurrent. Theoretically the difference between the redox potential of the redox couple I^-/I^-_3 and the Fermi level of TiO_2 under light illumination gives the value of open circuit voltage V_{oc}. The positive shift of conduction band edge upon addition of co-adsorbents $TiCl_4$ and CDCA should lead to a decrease in V_{oc}. However, a slight increase in the V_{oc} was observed after co-adsorption. It can be stated that sometimes, the occurrence of CDCA can also give rise to increased photovoltage, which can be attributed to the suppression of charge recombination[40]. The negative shift in conduction band edge or suppression of charge recombination is linked to the increment in V_{oc}. As a result, the loss of V_{oc} can be compensated by the suppression of charge recombination. Consequently this gives rise to increment in V_{oc} due of proton exchange from CDCA to the TiO_2 surface[41]. It is clear from the Table 1 that there is an appreciable amount of improvement in short current density and little effect on fill fac-

Table 1. Photovoltaic parameters of the fabricated DSSC

Device configuration	Device name	V_{oc} (Volt)	J_{sc} (mA/cm^2)	Fill factor	Efficiency η (%)
Untreated	D1	0.40	0.450	0.47	0.13
CDCA treated	D2	0.42	0.675	0.49	0.21
$TiCl_4$ + CDCA treated	D3	0.49	0.904	0.51	0.35

tors in successive steps of treatments. The overall power conversion efficiencies for devices D2 and D3 have been found to be improved significantly. This can be attributed the both conduction band edge lowering as well as reduced dye aggregation after both treatments. The short circuit current density J_{sc} was found to be 0.450 mA/cm^2, 0.675 mA/cm^2 and 0.904 mA/cm^2 for devices D1, D2 and D3 respectively. After treatment with CDCA and $TiCl_4$, the short circuit current density J_{sc} for device D3 was found to be almost double in magnitude as compared to that of untreated device D1. This can be attributed to the enhanced absorption in longer wavelength region due to lowering in TiO_2 conduction band edge and reduced dye aggregation which promoted the higher dye loading after surface treatment of the working electrode. The increased fill factor indicates the better quality of the cell after treatments. These results imply that improvement in conversion efficiency of DSSCs; based on natural dye quercetin, is due to increased short circuit current density J_{sc} and CDCA + $TiCl_4$ treatment is more significant than CDCA treatment towards enhancing the J_{sc}.

Conclusion

The study of UV-Vis spectra indicates that CDCA has been successful in reducing the dye aggregation which was evident by improved absorption. And lowering of conduction band can be attributed to the use of $TiCl_4$, which resulted photon harvesting in longer wavelength. Because of these reasons, a considerable improvement was observed in photo current delivered by the devices D2 and D3 both. The addition of co-adsorbents increased the effective surface area of the TiO_2 which resulted in higher dye loading giving rise to improved efficiency of devices.

The efficiencies of fabricated cells were not found to be very high. The possible grounds may be the low interaction between quercetin and the synthesized TiO_2, since the interaction between TiO_2 and the dye is very significant factor which affects the efficiency of DSSCs. Moreover; dyes extracted from natural resources suffer from low V_{oc}. The efficiency of DSSCs based on quasi solid polymeric electrolyte is also found to be less than DSSCs based on liquid electrolyte, which can be compensated in terms of durability.

References

1. B. K. Lee and J. J. Kim, *Current Applied Physics*, 2009, **9**, 404.
2. B. O'Regan and M. Grätzel, *Nature*, 1991, **353**, 737.
3. N. Robertson, *Angew. Chem., Int. Ed.*, 2006, **45**, 2338.
4. P. Wang, S. M. Zakeeruddin, R. H. Baker, J. E. Moser and M. Grätzel, *Adv. Mater.*, 2003, **15**, 2101.
5. H. J. Snaith and L. Schmidt-Mende, *Adv. Mater.*, 2007, **19**, 3187.
6. G. Boschloo, L. Haggman and A. Hagfeldt, *J. Phy. Chem. B*, 2006, **110**, 13144.
7. A. Mishra, M. K. R. Fischer and P. Bauerle, *Angew. Chem., Int. Ed.*, 2009, **48**, 2474.
8. G. Li, Y. Zhou, X. Cao, P. Bao, K. Jiang, Y. Lin and L. Yang, *Chem. Commun.*, 2009, **0**, 2201.
9. Z.-S. Wang, N. Koumura, Y. Cui, M. Takahashi, H. Sekiguchi, A. Mori, T. Kubo, A. Furube and K. Hara, *Chem. Mater.*, 2008, **20**, 3993.
10. P. Wang, S. M. Zakeeruddin, P. Comte, R. Charvet, R. Humphry Baker and M. Grätzel, *J. Phys. Chem. B*, 2003, **107**, 14336.
11. B. C. O'Regan, J. R. Durrant, P. M. Sommeling and N. J. Bakker, *J. Phys. Chem. C*, 2007, **111**, 14001.
12. K. Kakiage, Y. Aoyama, T. Yano, K. Oya, J. Fujisawab and M. Hanaya, *Chem. Commun.*, 2015, **51**, 15894.
13. T. Funaki, M. Yanagida, N. O. Komatsuzaki, Y. Kawanishi, K. Kasuga and H.Sugihara, *Inorg. Chim. Acta*, 2009, **362**, 2519.
14. Z. Ninq, Q. Zhang, W. Wu, H. Pei, B. Liu and H. Tian, *J. Org. Chem.*, 2008, **73**, 3791.
15. S. Ito, S. M. Zakeeruddin, R. H. Baker, P. Liska, R. Charvet *et al., Adv. Mat*er., 2006, **18**, 1202.
16. C. L. Wang, Y. C. Chang, C. M. Lan, C. F. Lo, E. W. G. Diau and C. Y. Lin, *Energy Environ Sci.*, 2011, **4**, 1788.
17. H. N. Tsao, J. Burschka, C. Yi, F. Kessler, M. K. Nazeeruddina and M. Grätzel, *Energy Environ. Sci.*, 2011, **4**, 4921.
18. M. A. S. García, X. Bokhimi, S. V. Martínez and A. E. J. González, *J. Nanotechnol.*, 2018 **1**. DOI:10.1155/2018/1236878
19. A. Kay and M. Grätzel, *J. Phys. Chem.*, 1993, **97**, 6272.
20. G. P. Smestad and M. Grätzel, *J. Chem. Edu.*, 1998, **75**, 752.
21. S. Hao, J. Wu, Y. Huang and J. Lin, *Sol. Energy*, 2006, **80**, 209.

22. A. S. Polo and N. Y. M. Iha, *Sol. Energy Mater. Sol. Cells*, 2006, **90**, 1936.
23. M. S. Roy, P. Balraju, M. Kumar and G. D. Sharma, *Sol. Energy Mater. Sol. Cells*, 2008, **92**, 909.
24. M. R. Narayan, *Renew. & Sust. Ene. Rev.,* 2012, **16**, 208.
25. H. Zhou, L. Wu, Y. Gao and T. Ma, *J. Photochem. Photobiol. A*, 2011, **219**, 188.
26. M. O. Karakus, I. Koca, O. Er and H. Çetin, *Optical Materials*, 2017, **66**, 552.
27. M. I. Bachtiar, M. N. P. Agustina, L. W. Hariyani and F. Nurosyid, *J. Phys. Conf. Series*, 2019, **1153**, 012097.
28. H. S. E.Ghamri, S. A. Taya, T. M. E. Agez, A. M. A. Kahlout, N. A. Dahoudi and M. S. A. Latif, *J. Nano and Elect. Phys.,* 2015, **7**, 03001.
29. O. Adedokun, M. K. Awodele, Y. K. Sanusi and A. O. Awodugba, IOP Conf. Series: Earth and Environmental Science, 2018, **173**, 012040.
30. S. Çakar and M. Özacar, *J. Photochem. Photobiol. A: Chem*., 2017, **346**, 512.
31. S. Sönmezoglu, C. Akyürek and S. Akin, *J. Phys. D: Appl. Phys*., 2012, **45**, 1.
32. Y. Li, G. Ma, S. Peng, G. Lu and S. Li, *Appl. Surf. Sci*., 2008, **254**, 6831.
33. K. F. Chen, C. H. Liu, H. K. Huang, C. H. Tsai and F. R. Chen, *Int. J. Electrochem. Sci*., 2013, **8**, 3524.
34. M. A. Ali, S. Srivastava, P. R. Solanki, V. V. Agrawal, R. John and B. D. Malhotra, *Appl, Phys. Lett.,* 2012, **101**, 084105.
35. S. N. Karthick, K. Prabakar, A. Subramania, J. T. Hong, J. J. Jang and H. J. Kim, *Powder Technology*, 2011, **205**, 36.
36. M. J. Šćepanović, M. G. Brojčin, Z. D. D. Mitrović and Z. V. Popović, *Science of Sintering,* 2009, **41**, 67.
37. N. G. Park, J. Lagemaat and A. J. Frank, *J. Phys. Chem. B*, 2000, **104**, 8989.
38. J. Zhang, P. Zhou, J. Liub and J. Yu, *Phys. Chem. Chem. Phys*., 2014, **16**, 20382.
39. A. Kay and M. Grätzel, *J. Phys. Chem.,* 1993, **97**, 6272.
40. L. Jing, W. W. Jun, Y. J. Bao, T. Jin, L. Y. Tao and H. J. L, *Sci. Ch. Chem*., 2011, **54**, 699.
41. G. D. Sharma, R. Kurchania, R. J. Ball, M. S. Roy and J. A. Mikroyannidis, *Int. J. Photoenergy*, 2012. DOI: 10.1155/2012/983081.